


# Energy focusing of flexural waves via algorithmically optimized coding metasurface lenses

Zi-Rui Wang(王子睿), Di-Chao Chen(陈帝超), Rui Hong(洪瑞), and Da-Jian Wu(吴大建)
**Citation:**Chin. Phys. B, 2025, 34 (**9**): 094302. DOI: 10.1088/1674-1056/add1be
http://cpb.iphy.ac.cn; http://iopscience.iop.org/cpb

**What follows is a list of articles you may be interested in**

---

## Overcoming bandwidth limitations in space-coiled acoustic metamaterials through inclined perforated plate design

Jixin Liu(刘继鑫), Fengmin Wu(吴丰民), Ting Li(李婷), Junjun Wang(王军军), Xinye Zou(邹欣晔), and Dong Zhang(章东)
Chin. Phys. B, 2025, 34 (**1**): 014303. DOI: 10.1088/1674-1056/ad8fa2

## High-efficiency wide-angle anomalous refraction with acoustic metagrating

Kangyao Sun(孙康瑶), Yuancheng Fan(樊元成), Zhehao Ye(叶哲浩), Jiahui Li(李嘉荟), Quanhong Fu(付全红), Yali Zeng(曾雅丽), and Fuli Zhang(张富利)
Chin. Phys. B, 2025, 34 (**1**): 014302. DOI: 10.1088/1674-1056/ad8db6

## Orbital angular momentum conversion of acoustic vortex beams via planar lattice coupling

Qingbang Han(韩庆邦), Zhipeng Liu(刘志鹏), Cheng Yin(殷澄), Simeng Wu(吴思梦), Yinlong Luo(罗寅龙), Zixin Yang(杨子鑫), Xiuyang Pang(庞修洋), Yiqiu Wang(王溢秋), Xuefen Kan(阚雪芬), Yuqiu Zhang(张雨秋), Qiang Yu(俞强), and Jian Wu(吴坚)
Chin. Phys. B, 2024, 33 (**9**): 094301. DOI: 10.1088/1674-1056/ad57ad

## Pipeline thickness estimation using the dispersion of higher-order SH guided waves

Zhengchen Dai(代政辰), Jinxia Liu(刘金霞), Yunfei Long(龙云飞), Jianhai Zhang(张建海), Tribikram Kundu, and Zhiwen Cui(崔志文)
Chin. Phys. B, 2024, 33 (**7**): 074301. DOI: 10.1088/1674-1056/ad3033

## Sensing the heavy water concentration in an $H_2O$—$D_2O$ mixture by solid—solid phononic crystals

Mohammadreza Rahimi and Ali Bahrami
Chin. Phys. B, 2024, 33 (**4**): 044301. DOI: 10.1088/1674-1056/ad0bf5

---

# Energy focusing of flexural waves via algorithmically optimized coding metasurface lenses

Zi-Rui Wang(王子睿)[†], Di-Chao Chen(陈帝超)[†,‡], Rui Hong(洪瑞), and Da-Jian Wu(吴大建)[§]

*Institute of Acoustics, School of Physics and Technology, Nanjing Normal University, Nanjing* 210023, *China*

(Received 13 March 2025; revised manuscript received 15 April 2025; accepted manuscript online 29 April 2025)

Efficient elastic wave focusing is crucial in materials and physical engineering. Elastic coding metasurfaces, which are innovative planar artificial structures, show great potential for use in the field of wave focusing. However, elastic coding lenses (ECLs) still suffer from low focusing performance, thickness comparable to wavelength, and frequency sensitivity. Here, we consider both the structural and material properties of the coding unit, thus realizing further compression of the thickness of the ECL. We chose the simplest ECL, which consists of only two encoding units. The coding unit 0 is a straight structure constructed using a carbon fiber reinforced composite material, and the coding unit 1 is a zigzag structure constructed using an aluminum material, and the thickness of the ECL constructed using them is only 1/8 of the wavelength. Based on the theoretical design, the arrangement of coding units is further optimized using genetic algorithms, which significantly improves the focusing performance of the lens at different focus and frequencies. This study provides a more effective way to control vibration and noise in advanced structures.

**Keywords:** coding metasurface, elastic wave focusing, genetic algorithm

**PACS:** 43.40.+s, 46.15.Cc, 46.40.–f

**DOI:** 10.1088/1674-1056/add1be **CSTR:** 32038.14.CPB.add1be

## 1. Introduction

In large weigh beam, plate, and shell structures such as bridges, floor slabs, and wings, the majority of structural noise propagates in the form of elastic waves.[1,2] To reduce or even eliminate noise interference, effective control of elastic waves needs to be realized. The emergence of metamaterials has provided an effective means of controlling elastic waves, and the use of metamaterials has enabled the realization of a large number of anomalous physical phenomena that are not possible with natural materials,[3–5] such as negative equivalent mass and negative bulk modulus,[6–9] invisibility cloaks,[10–12] and perfect acoustic absorption.[13,14] The bandgap effect of locally resonant[15,16] or inertially amplified metamaterials[17,18] can be utilized to shield elastic waves in certain specific frequency regions. Placing these metamaterial structures between the noise source and the building prevents noise by reflecting or absorbing the propagating elastic waves.[19] However, such an approach makes the potential energy carried by the noise not effectively utilized and is a waste of energy.

The energy carried by noise or waves is a form of clean energy that is characterized by its absence of pollution. The utilization of this energy and the transformation of waste into valuable resources are subjects of significant importance in both academic research and engineering applications. Harvesters are suitable devices for capturing energy from structural vibrations and converting it into electricity for various applications. To ensure its effective collection of noise or wave energy, the phenomenon of wave focusing needs to be realized first.[20] The prioritization of elastic wave focusing as energy harvesting can permit rational arrangement of harvesters.[21,22] In recent years, the study of elastic ultrathin metamaterials, also known as metasurfaces,[23–26] has facilitated the development of techniques such as elastic wave focusing.[27–29] For the sake of simplicity in production, the most basic elastic coding metasurfaces need only have elements of two types corresponding to the 0 and $\pi$ phases.[30–33] However, the limitation of the number of coding unit types leads to the low focusing performance of the elastic coding lens (ECL). In addition, ECLs typically have a thickness comparable to the wavelength and are frequency sensitive, which also limits their further application in practice. Therefore, the current issues that require urgent attention include the focusing performance, thickness, and operating frequency of the ECL.

In this work, we choose ECLs constructed from two coding unit types. Further compression of the ECL thickness is achieved by simultaneously considering the structural and material properties of the coding unit. The coding unit 0 is a straight structure constructed using a carbon fiber reinforced composite material, and the coding unit 1 is a zigzag structure constructed using an aluminum material. Based on the theoretical design, the optimal arrangement of the proposed

[†]These authors contributed equally to this work.

[‡]Corresponding author. E-mail: chendichao@njnu.edu.cn

[§]Corresponding author. E-mail: wudajian@njnu.edu.cn

© 2025 Chinese Physical Society and IOP Publishing Ltd. All rights, including for text and data mining, AI training, and similar technologies, are reserved.

coding units is investigated using a genetic algorithm. Simulation results verify the excellent performance of the ECL in elastic wave focusing after the optimized coding unit arrangement. Furthermore, based on the genetic algorithm, we can optimize the arrangement of the coding units that make up the ECL, thus achieving efficient elastic wave focusing at different operating frequencies.

## 2. Theoretical framework

Figure 1(a) shows a schematic diagram of the focusing of an elastic wave through an ECL. The designed ECL consists of two types of coding units (defined as coding units 0 and 1). The coding units 0 and 1 have high transmission amplitudes and simultaneously satisfy a phase difference of $\pi$. An ECL consisting of a single coding unit can also achieve elastic wave focusing. Compared to it, the ECL composed of two types of coding units produces greater focusing intensity and enables more precise control of the focus position. According to the Huygens–Fresnel principle, a proper arrangement of coding units 0 and 1 can focus a vertically incident elastic wave at a predetermined position. In order for an elastic wave to produce constructive interference at the focused position, the phase difference between two adjacent positions on the ECL should be $\pi$. This implies that the wave range difference must satisfy

$$l_{\pm(i+1)} - l_{\pm i} = \frac{\lambda}{2}, \tag{1}$$

where $l_{\pm i} = \sqrt{f_y^2 + (f_x - x_{\pm i})^2}$ $(i = 0, 1, 2, \ldots)$ is the wave path of the elastic wave from the center of position $x_i$ to the focus, $x_i$ is the horizontal distance from the center position to the center of the ECL, $\lambda = c_{\mathrm{A}}/f$ is the wavelength, $f$ is the operation frequency. $c_{\mathrm{A}}$ denotes the propagation speed of the waves in the host plate (aluminum), which can be expressed as

$$c_{\mathrm{A}} = \left[E\omega^2(H/2)^2/3\rho(1-\upsilon^2)\right]^{1/4}, \tag{2}$$

where $H$ is the thickness of the plate, $\omega = 2\pi f$ is the angular frequency, $E$, $\rho$, and $\nu$ are the elastic modulus, mass density, and Poisson's ratio, respectively, each of which is constant for any given material. From Eq. (1), we can obtain the recursive formula between adjacent positions

$$x_{\pm(i+1)} = \pm\left(\sqrt{\left(\frac{\lambda}{2} + \sqrt{f_y^2 + (f_x - x_{\pm i})^2}\right)^2 - f_y^2} \pm f_x\right). \tag{3}$$

Coding units 0 and 1 are placed in two adjacent positions to ensure that constructive interference is generated at the focusing position. Here, we place coding unit 0 at the center of the ECL, coding unit 1 at an adjacent position, and so on. Coding units 0 and 1 occupy two rectangular regions with the same length and width, and their lengths and widths are $h = 3.6$ mm and $t = 6$ mm, respectively, as shown by the green and red rectangular boxes in Fig. 1(a). Previous designs[29] have shown that it is possible to convert an elastic wave from the $S_0$ mode to the $A_0$ mode using a resonant unit to achieve full coverage of the $2\pi$ propagation phase. However, this results in a low power of the transmitted wave. Therefore, we design ECLs with negligible mode conversion, which can realize the modulation of asymmetric flexural wave ($A_0$ mode) wavefronts. Coding units 0 and 1 consist of two different materials. The material selected for coding unit 1 is aluminum, which is the same as the material of the plate. An isotropic homogeneous material with a high Young's-modulus-to-mass-density ratio is selected for coding unit 0. Carbon fiber reinforced composites are used here. Other materials can also be used for coding unit 0 as long as they have a higher Young's-modulus-to-mass-density ratio than aluminum, and the thickness of the ECL can be further compressed by choosing the right material. The Young's modulus, Poisson's ratio, and mass density of aluminum are 70 GPa, 0.33, and 2700 kg·m$^{-3}$, respectively. The Young's modulus, Poisson's ratio, and mass density of carbon fiber reinforced composites are 500 GPa, 0.31, and 2000 kg·m$^{-3}$, respectively.[26] In addition to the choice of material, the delay of the transmitted phase of the flexural wave can be realized by changing the shape structure of the coding unit. The zigzag structure has a longer propagation distance compared to a straight bar, which is used as coding unit 1 to provide a larger phase delay. The increase in the folding width $b$ of the zigzag structure can further compress the thickness of the ECL, but this also leads to an increase in the width of the individual coding units, which is not conducive to accurate bending wave focusing. Here, the operating frequency of the incident wave is set to 74 kHz. The inset of Fig. 1(a) shows a schematic diagram of coding units 0 and 1. The coding unit 0 with a straight bar has a structure width $a = 1$ mm, the coding unit 1 with a zigzag structure has a notch spacing $s = 1$ mm and a folding width $b = 4.6$ mm. The flexural wave will propagate along the straight or zigzag structure when it passes through the ECL consisting of coding unit 0 and coding unit 1. Since there is no contact surface between adjacent coding units, the interaction between adjacent units is negligible. In addition, edge effects are negligible when the focal point is far from the ECL. Based on full-wave numerical simulations with the finite element software, we investigate the transmission amplitude and phase of the coding units. Figure 1(b) shows a model of a strip with coding units. A perfectly matched layer (PML) is used at both ends of the strip model to simulate infinite boundary and to absorb all transmitted waves beyond this point, thus avoiding the influence of flexural wave reflections on the results. In the finite element software, the coding unit and strip models are modelled using free tetrahedral meshes with user-defined element size. The maximum and minimum element sizes are 2 mm and 0.1 mm, respectively. The PML is discretized using a scanning mesh, with the number of distribution layers being

20. The thickness $H$ of the strip model is set to 5 mm, and the same free tetrahedral mesh is used for modelling in the thickness direction, and the transmitted waves are travelling waves in the $A$ mode. Apply continuous periodic boundary conditions to both sides of the strip model. An initial excitation along the $z$-direction is applied to the left side of the strip model to generate an incident flexural wave. The displacement phase shift of the $z$-component of the flexural wave transmitted through the coding unit can be detected by a probe line placed in the far field. The transmission ratio formula can be expressed as[28]

$$T = \iint_{S_2} |A|\,\mathrm{d}s \Big/ \iint_{S_1} |A|\,\mathrm{d}s, \tag{4}$$

where $|A|$ is the out-of-plane displacement, and the $S_1$ and $S_2$ regions are areas of the same size before and after the coding unit, respectively. The amplitude and relative phase shift of the flexural wave as a function of frequency after passing through coding units 1 and 0 are illustrated in Fig. 1(c). It can be observed that the phase difference between coding units 0 and 1 at 74 kHz is approximately $\pi$, which satisfies our design requirements. In addition, the transmission amplitudes of coding units 0 and 1 at 74 kHz are approximately equal, both close to 0.9, which facilitates the ECL to achieve focus. The transmission amplitude of coding unit 1 is highest at 77.2 kHz, but at this point the phase difference between coding units 0 and 1 is $1.2\pi$ and the difference in transmission amplitude is large compared to that at 74 kHz. Actually, from 74 kHz to 75 kHz, coding units 0 and 1 can well meet the required transmission amplitude and phase difference, but the flexural wave has the longest wavelength at 74 kHz, which we chose to select in view of the need for a thinner thickness of the ECL. To provide a more detailed illustration of the working mechanism, a simulation of the out-of-plane displacement field corresponding to the flexural wave generated by coding units 1 and 0 at 74 kHz is presented in Fig. 1(d).

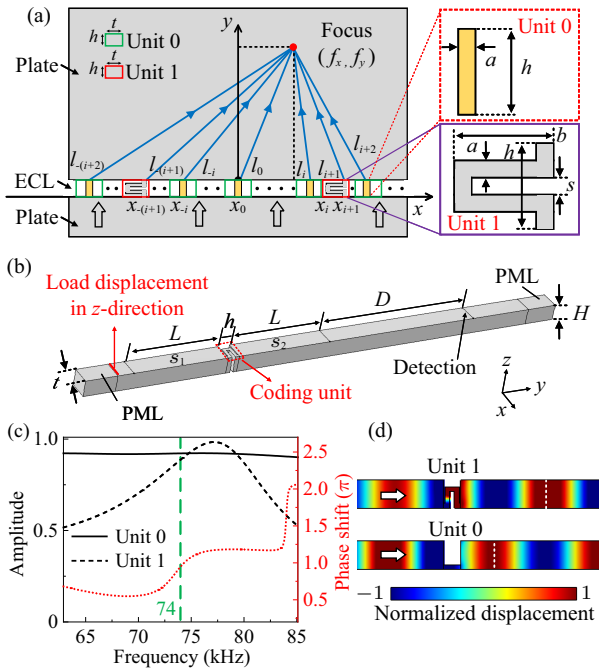



**Fig. 1.** (a) Schematic diagram of elastic wave focusing by using elastic coding lens (ECL) with coding units 1 and 0. (b) Schematic diagram of the strip model for a single coding unit. (c) Variation of transmission amplitude and relative phase shift with frequency. (d) Simulated out-of-plane displacement field produced by the coding units 1 and 0.

## 3. Implementation and optimization

The ECL is a collection of two coding units that are distributed parallel to each other in the direction of propagation perpendicular to the incident flexural wave and connected at both ends to plates. Focusing of flexural waves can be realized by adjusting the arrangement of coding units. We first verify that the focusing on the central axis of the ECL ($f_x = 0$), at which case equation (3) simplifies to

$$x_{\pm(i+1)} = \pm\left(\sqrt{\left(\frac{\lambda}{2} + \sqrt{f_y^2 + x_{\pm i}^2}\right)^2 - f_y^2}\right). \tag{5}$$

The focus is set to $(x, y) = (f_x, f_y) = (0, 53\ \mathrm{mm})$. The ECL consists of 31 coding units, and the total length of the ECL will limit the range of focus. As the total length of the ECL increases, the number of adjacent positions will increase, and the adjustable range of focus will increase accordingly. Conversely, as the total length of the ECL decreases, the number of adjacent positions decreases, which reduces the adjustable range of focus and even affects focus formation. The arrangement of the coding units and the transmitted intensity field they realize are shown in Fig. 2(a). The flexural wave propagates from the bottom toward the ECL, and most of the transmitted energy converges to a finite-length region on the central axis of the ECL. Here, we only consider the coding units in the adjacent positions, and the rest of the region is filled with coding unit 0. However, in the actual design the type of coding units in the remaining area also affects the intensity of the focus. Therefore, the type of coding units for the remaining regions needs to be carefully selected. When the number of codes is sufficiently large, the traditional parameter scanning approach is cumbersome, even when guided by empirical knowledge. This is a prototypical inverse design problem, the objective of which is to ascertain the optimal coding unit alignment from the intensity response of the target region. Accordingly, we have elected to adopt a genetic algorithm, a metaheuristic inspired by the rule of natural selection, for the purpose of optimizing the alignment of the coding units. Genetic algorithms, as evolutionary algorithms, not only overcome the local optimum pitfalls of gradient-based algorithms such as topological optimization and concomitant variable algorithms, but also do not necessitate the generation of a substantial number of well-labeled datasets, and thus can be used to solve problems with discrete parameters.[15,34] Figure 2(b) shows the optimization

process. The genetic algorithm starts with a randomly generated initial population of 200. We treat each coding unit as a gene, and they form a chromosome encoded by binary-valued genes, the designed ECL. The transmittance and phase shift of coding units 0 and 1 at the operating frequency are input into the algorithm. We define the intensity in a circle centered on the target focus position in the working plane with a radius of 1 mm as the fitness function. The parameters corresponding to each chromosome are input into the finite element simulation software, where the corresponding ECLs are generated and numerically simulated. The intensity at the target location obtained from the numerical simulation is passed back to the genetic algorithm. The fitness of each candidate solution is numerically evaluated and ranked by computing all chromosomes. If the results converge or the iteration reaches the maximum number of generations, the program is stopped; otherwise the chromosomes within the population are subjected to operations such as crossover interchanges, mutations, etc. and the fitness values are evaluated again until the results converge or the maximum number of iterations is reached. Figure 2(c) shows the optimized ECL arrangement and the corresponding transmitted intensity field. It can be seen that the focusing intensity achieved by the ECL after optimizing the arrangement of the coding units can reach 2.4 times that before optimization. We show the intensity distribution along dashed lines "I" and "III" in Fig. 2(d) and along dashed lines "II" and "IV" in Fig. 2(e). To better compare the focusing intensities before and after EPL optimization, we normalize the intensity fields in Figs. 2(d) and 2(e). The full width at half maximum (FWHM) of the flexural wave focusing before and after the EPL optimization is about $0.47\lambda$ and $0.42\lambda$, respectively, and the focusing intensity produced by the ECL before the optimized arrangement is only 0.42 of the optimized one, as shown in Fig. 2(d). The depth of focus before and after EPL optimization is about $1.69\lambda$ and $1.84\lambda$, respectively. Meanwhile the focus positions obtained before and after the EPL optimization are $(x,y) = (f_x, f_y) = (0, 52\ \text{mm})$ and $(x,y) = (f_x, f_y) = (0, 53\ \text{mm})$, respectively, as shown in Fig. 2(e), which are both consistent with the theoretical design.

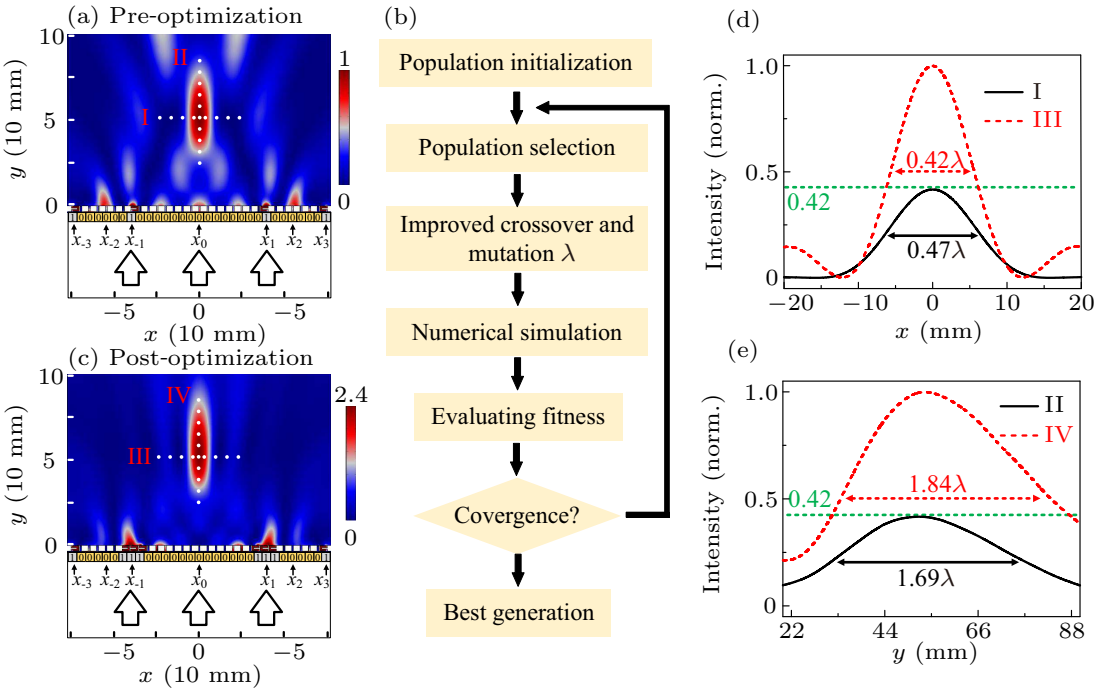



**Fig. 2.** (a) Focusing intensity field distribution by unoptimized ECL. (b) Flow graph of the genetic algorithm. (c) Focusing intensity field distribution by optimized ECL. Intensity profiles on (d) the lines "I" and "III", and (e) the lines "II" and "IV".

Next, we change the position of the focus by changing the arrangement of the coding units. The first demonstration is the modulation of the focal length. Change the focus of the ECL to $(f_x, f_y) = (0, 17\ \text{mm})$. Based on Eq. (5), we obtain the initial arrangement of coding units on the ECL. Then we optimize it using a genetic algorithm and the arrangement of coding units on the ECL after optimization is shown in Fig. 3(a). It can be seen from the transmitted intensity field that the optimized ECL achieves effective focusing of flexural waves. Figures 3(b) and 3(c) show the focusing intensity distributions along the "I" and "II" dashed lines, respectively. The red dashed line indicates the distribution of focusing intensity produced by the conventional ECL before the optimized arrangement, whose maximum intensity is only 0.34 of the optimized one. The focus positions obtained from numerical simulations before and after optimization are both $(f_x, f_y) = (0, 17\ \text{mm})$, which are consistent with the theoretical settings. It can also be seen that the FWHM of the focus before and after optimization is about $0.37\lambda$ and $0.33\lambda$, respectively, and the depth of focus is $0.84\lambda$ for both.

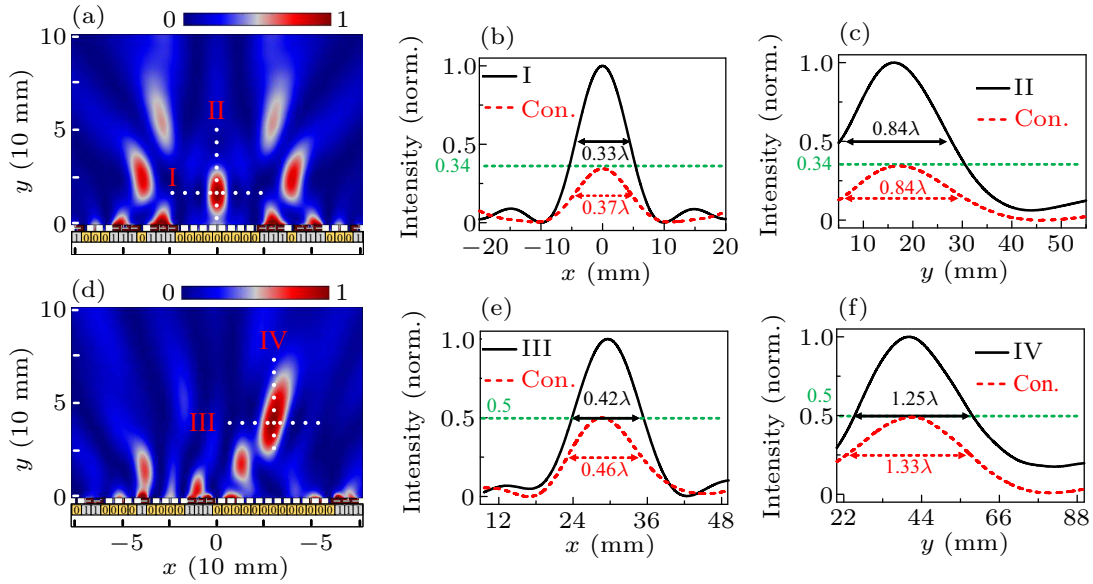



**Fig. 3.** (a) Intensity field distribution for axial focusing achieved by the optimised ECL. Intensity profiles along (b) dotted line "I" and (c) dotted line "II". (d) Intensity field distribution for off-axis focusing achieved by the optimized ECL. Intensity profiles along (e) dotted line "III" and (f) dotted line "IV". The red dashed line indicates the distribution of focusing intensity produced by the unoptimized ECL.

Second, we realized off-axis focusing by changing the arrangement of coding units. Set the off-axis focus coordinates to $(f_x, f_y) = (30\ \text{mm}, 40\ \text{mm})$. Based on Eq. (3) and the genetic algorithm, we obtain the positional parameters of the optimized coding units and simulated intensity distributions, as shown in Fig. 3(d). The vertically incident flexural wave produces off-axis focusing after passing through the ECL. Figures 3(e) and 3(f) show the focusing intensity distributions along the dashed lines "III" and "IV" near the focus, respectively. The red dashed line indicates the focusing intensity distribution before the optimized arrangement, whose maximum intensity is only 0.5 of the optimized one. The focus positions obtained from numerical simulations before and after the optimized arrangement are $(f_x, f_y) = (30\ \text{mm}, 40\ \text{mm})$ and $(f_x, f_y) = (29\ \text{mm}, 41\ \text{mm})$, respectively, which are consistent with the theoretical design. The above simulation results show that the designed subwavelength ECL is able to maximize the focus intensity while achieving precise control of the focus position.

Finally, we further investigate the effect of the optimization method on the frequency response characteristics of the ECL. From Fig. 1(c), it can be seen that the relative phase shift of the coding unit varies between $0.5\pi$ and $2\pi$ as the frequency increases from 62.9 kHz to 85.1 kHz (15% fluctuation in operating frequency). At 62.9 kHz and 85.1 kHz, the transmission amplitudes of the coding unit 1 are 0.51 and 0.52, respectively, and the relative phase shifts of the two coding units are $0.68\pi$ and $2.06\pi$, respectively.

The transmission intensity distribution after changing the operating frequency of the incident flexural wave in Fig. 2(a) to 62.9 kHz is shown in Fig. 4(a1). The focusing effect deteriorates because the transmission amplitude and relative phase shift of the coding unit are changed. Based on the genetic algorithm, the arrangement of the coding units of the ECL is optimized. Figure 4(a2) shows the coding unit arrangement of the optimized arrangement of the ECL and the transmission intensity distribution at 62.9-kHz frequency. Figures 4(b1) and 4(b2) show the intensity distributions for dashed lines "I", "III", and dashed lines "II", "IV", respectively. It is seen that the maximum value of intensity produced by the conventional ECL before the optimized arrangement is only 0.62 of the intensity after the optimization. Meanwhile, the focus position before optimization deviates from the theoretical prediction, and the focus position produced by the ECL after optimization is $(f_x, f_y) = (0, 51\ \text{mm})$, which is consistent with our theoretical design. Figures 4(c1) and 4(c2) show the transmission intensity distribution of the ECL before and after the optimized arrangement at 85.1-kHz frequency, respectively. Figures 4(d1) and 4(d2) show the intensity distributions for dashed lines "V", "VII", and dashed lines "VI", "VIII", respectively. The maximum value of the focusing intensity produced by the conventional ECL before the optimized arrangement is only 0.18 of the focusing intensity after the optimization. Thus, our proposed coding unit can be used to prepare ECLs with different operating frequencies. By optimizing the arrangement of the coding bits, the focusing position can be corrected while further enhancing the focusing intensity at the focusing position.

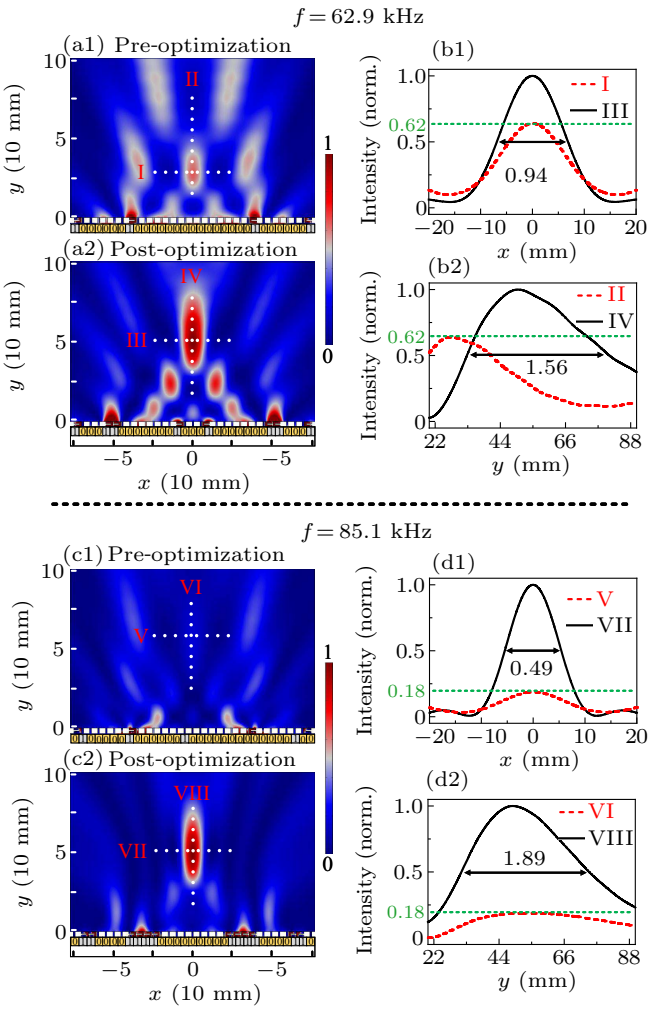



**Fig. 4.** Focusing intensity field distribution by (a1) unoptimized ECL and (a2) optimized ECL at $f = 62.9$ kHz. Intensity profiles on (b1) the lines "I" and "III", and (b2) the lines "II" and "IV". Focusing intensity field distribution by (c1) unoptimized ECL and (c2) optimized ECL at $f = 85.1$ kHz. Intensity profiles on (d1) the lines "V" and "VII", and (d2) the lines "VI" and "VIII".

## 4. Conclusion

The simplest ECL is used to realize effective elastic wave focusing. The optimization of the arrangement of coding units using genetic algorithms improves the focusing performance of ECLs. In the configuration, coding unit 0 is a straight carbon fiber reinforced composite structure, and coding unit 1 is a zigzag aluminum structure. The ECL constructed by these two coding units has a thickness of only 1/8 of the wavelength. We numerically simulate the ECL realization with different focal lengths and off-axis focusing cases. Simulation results verify the excellent performance of the proposed ECL in focusing elastic waves at arbitrary positions. Finally, we optimize the coding unit arrangement of ECL based on a genetic algorithm to achieve efficient focusing at 62.9 kHz and 85.1 kHz.

## Acknowledgements

Project supported by the National Natural Science Foundation of China (Grant No. 12404531) and the Natural Science Foundation of the Higher Education Institutions of Jiangsu Province, China (Grant No. 23KJB140011).

## References

[1] Zhu H, Patnaik S, Walsh T F, Jared B H and Semperlotti F 2020 *Proc. Natl. Acad. Sci. USA* **117** 26099
[2] Li P, Qian Z, Zhang Y, Ma T, Kuznetsova I E, Qian Z and Kolesov V 2023 *Energy* **267** 126523
[3] Wang G, Wen X, Wen J, Shao L and Liu Y 2004 *Phys. Rev. Lett.* **93** 154302
[4] Danawe H and Tol S 2022 *J. Sound Vib.* **518** 116552
[5] Liu Y, Liang Z, Liu F, Diba O, Lamb A and Li J 2017 *Phys. Rev. Lett.* **119** 034301
[6] Liu Z, Zhang X, Mao Y, Zhu Y Y, Yang Z, Chan C T and Sheng P 2000 *Science* **289** 5485
[7] Huang H H, Sun C T and Huang G L 2009 *Int. J. Eng. Sci.* **47** S69
[8] Fang N, D, Xu J, Ambati M, Srituravanich W, Sun C and Zhang X 2006 *Nat. Mater.* **5** 6
[9] Liu Y, He Z, Yang Y, Li X, Li Z and Ma H 2022 *Biosens. Bioelectron.* **211** 114392
[10] Zhang S, C and Fang N 2011 *Phys. Rev. Lett.* **106** 024301
[11] Yang T, Bai X, Gao D, Wu L, Li B, Thong J T and Qiu C W 2015 *Adv. Mater.* **27** 7752
[12] Chen H, Wu B I, Zhang B and Kong J A 2007 *Phys. Rev. Lett.* **99** 063903
[13] Wang X, Luo X, Zhao H and Huang Z 2018 *Appl. Phys. Lett.* **112** 021901
[14] Long H, Zhu Y, Gu Y, Cheng Y and Liu X 2022 *Phys. Rev. Appl.* **18** 044032
[15] Ma G and Sheng P 2016 *Sci. Adv.* **2** e1501595
[16] Oudich M, Li Y, Assouar BM and Hou Z 2010 *New J. Phys.* **12** 083049
[17] Hussein M I, Patrick I, Banerjee A and Adhikari S 2022 *J. Sound Vib.* **531** 116977
[18] Banerjee A, Adhikari S and Hussein M I 2021 *Int. J. Mech. Sci.* **207** 106630
[19] Zhu H, Walsh T F and Semperlotti F 2018 *Appl. Phys. Lett.* **113** 221903
[20] Li J, Zhou Y and Chen H 2023 *Chin. Phys. B* **32** 064201
[21] Li P, Qian Z, Dong B, Qian Z, Ma T and Kuznetsova I 2023 *Int. J. Mech. Sci.* **248** 108206
[22] Liu Y Q, Sun J, Shu Y, Wu L, Lu L, Qi K, Che Y, Li L and Yin H 2021 *Opt. Lasers Eng.* **147** 106734
[23] Hu Y, Li M, Liu H and Li B 2023 *Eng. Struct.* **262** 114392
[24] Kildishev A V, Boltasseva A and Shalaev V M 2013 *Science* **339** 6125
[25] Ma G, Yang M, S, Yang Z and Sheng P 2014 *Nat. Mater.* **13** 9
[26] Zhang J, Su X, Liu Y, Zhao Y, Y and Hu N 2019 *Int. J. Solid Struct.* **162** 14
[27] Lin Z, Xu W, Xuan C, Qi W and Wang W 2021 *J. Phys. D: Appl. Phys.* **54** 255303
[28] Yang T, Lin Z, Zhu X and Yang T 2022 *Phys. Rev. Appl.* **18** 064065
[29] Zhu H and Semperlotti F 2016 *Phys. Rev. Lett.* **117** 034302
[30] Chen D C, Zhu X F, Wei Q, Yao J and Wu D J 2020 *J. Phys. D: Appl. Phys.* **53** 255501
[31] Zhang N L, Zhao S D, Dong H W, Wang Y S and Zhang C 2022 *Appl. Phys. Lett.* **120** 142201
[32] W Li W, Meng F and Huang X. 2020 *Appl. Phys. Lett.* **117** 021901
[33] Liu F Y, Zhang N L, Dong H W, Wang F J and Zhao S D 2023 *Appl. Phys. Lett.* **123** 011706
[34] He Z, Yuan K, Xiong G and Wang J 2023 *Chin. Phys. Lett.* **40** 104402